Bull Earthquake Eng (2010) 8:897–919
DOI 10.1007/s10518-010-9173-y

ORIGINAL RESEARCH PAPER

Application of direct displacement based design to long span bridges

Gopal Adhikari · Lorenza Petrini · Gian Michele Calvi

Received: 10 October 2008 / Accepted: 14 January 2010 / Published online: 2 February 2010

Abstract The paper investigates the applicability of current direct displacement based seismic design (DDBD) procedure, developed by Priestley and his coworkers, for straight long span bridges under transverse seismic excitation synchronous to all supports. This category of bridges often possess some additional features such as massive tall piers, highly irregular distribution of mass and stiffness due to unequal superstructure spans and pier heights, large deformation capacity etc. that are absent in short-to-moderate span bridges for which DDBD has extensively been verified. It is shown that DDBD in its current form is unable to capture both displacement and base shear demand when compared with nonlinear dynamic analysis results. Accordingly, a simple mechanics based extension of the current procedure that takes into account the effect of pier mass while computing base shear demand as well as a modal combination rule for estimating displacement demand is proposed and validated using a series of parametric studies. The new procedure also allows engineer to allocate strength at the potential plastic hinge location in more general terms.

Keywords Seismic design · Displacement-based approach · Fore-based approach · Long span bridges

G. Adhikari
European School for Advanced Studies in Reduction of Seismic Risk (ROSE School), Via Ferrata 1, 27100 Pavia, Italy
e-mail: gadhikari@roseschool.it

L. Petrini (✉)
Department of Structural Engineering, Politecnico di Milano, Piazza Leonardo da Vinci 32, 20133 Milano, Italy
e-mail: lorenza.petrini@polimi.it

G. M. Calvi
Department of Structural Mechanics, Università degli Studi di Pavia, Via Ferrata 1, 27100 Pavia, Italy

1 Introduction

In the last decade or so, a significant shift in the conceptual philosophy of research on earthquake resistant structures has been observed, due to the recognition of the primary role of displacement and deformation as more reliable and direct indices of structural (and non-structural) damage than strength, as considered earlier. The major drawbacks and possibly unconservative inconsistencies of the traditional force based design procedures have also been identified and well documented in the literature (Uang 1991; Priestley 2003; among others). Although the use of displacement as a design parameter can be traced back to the work of Muto et al. in 1960 (as reported by Moehle 1992), the major breakthrough came only after the publication of ATC-40 document (ATC 1996) and FEMA-273 guidelines (BSSC 1997), where an explicit definition of performance level, in terms of deformation to be expected for a specific hazard level, is given for the first time. Following this idea, researchers have developed a number of displacement controlled design procedures that allow the engineer to specify a certain level of deformation that a structural system achieves under the effect of a prescribed seismic hazard considering explicitly material inelasticity and geometric nonlinearity of the system. Among the recently developed displacement controlled procedures (Panagiatakos and Fardis 1999; Browning 2001; Aschheim and Black 2000; Freeman 1998) the direct displacement based design (DDBD) procedure developed by Priestley and his co-workers (Priestley et al. 2007) seems to be (Sullivan 2003) well equipped to address the deficiencies of conventional force based design, developed in a complete form and simple to apply. Historically, it was first developed for a single column bridge system (Kowalsky 2002) following the idea of 'Substitute structure' conceptualized by Shibata and Sozen (1976). Afterwards it was extended to other structural configurations also such as frame, structural wall and dual wall-frame buildings, isolated structures, etc. (Priestley et al. 2007). Regarding bridges, this procedure was successfully applied to short-to-moderate span bridges with continuous deck having various configurations of regular/ irregular pier heights and uniform span-lengths (Alvarez Botero 2004; Ortiz Restrepo 2006; and Priestley et al. 2007). The extension of the current framework of DDBD procedure to long span concrete bridges, however, requires some additional considerations because of some peculiar issues related to this category of bridges. The aim of this study is, therefore, to define such additional considerations that are required for long span concrete bridges with limited ductile piers (as in the case of a bridge crossing a deep valley) and with/without in-plan movement joints to allow seasonal movement (due to temperature) and long term deformation (due to creep and shrinkage of concrete).

Following a brief review of current state-of-the-art of the DDBD procedure, the issues related to long span bridges are identified and necessary modifications are proposed. The accuracy of the proposed modifications is then explored through comparison of results from a large number of nonlinear response history analyses. For the sake of completeness of the study, a comparison is also made between the results of DDBD after proposed modifications and traditional force-based design procedure.

2 DDBD: current state-of-the-art

The Direct Displacement Based Design (DDBD) can be defined as a response spectrum based approach, which utilizes the substitute structure methodology developed by Shibata and Sozen (1976) to model an inelastic system with equivalent linear elastic properties, such as equivalent elastic secant stiffness to the maximum response point and a consistent

equivalent viscous damping value utilizing Jacobsen's method modified for real ground motion records. Since the substitute structure is elastic, its response is also computed from an elastic response spectrum scaled to proper equivalent viscous damping. A detailed discussion on the fundamentals of DDBD and its application to different type of structures can be found elsewhere (Priestley et al. 2007). A recapitulation of major steps involved in the design of multi-span bridges is, however, presented below for the sake of completeness of this study. In particular, the response under transverse excitation is taken into account, considered that the longitudinal response of straight bridge is relatively simple as design and response displacements are the same for all the piers.

1. **Estimate the initial displacement profile.** This step involves choosing a displacement shape that represents the first inelastic mode shape[1] and determining the limit-state displacement capacities of the piers either from strain based criterion to limit structural damage or from drift based criterion to protect non-structural elements. In the present study, a half-sine based mode shape (Alvarez Botero 2004) along with a drift based criterion (taken as 0.035 radian (ATC/MCEER 1999)) is used to define the initial displaced profile of the bridge. Use of drift based criterion eliminates the need of sectional analysis as required for strain based criterion to define target displacement of each pier. Furthermore, in case of tall piers, it is difficult to reach their ultimate displacement capacity and hence an approximate calculation by limiting drift ratio is sufficient.
2. **Define an equivalent SDOF structure.** In this step, an equivalent SDOF system, represented by a system displacement (Eq. 1) and a system mass (Eq. 2), is established by equating the work done by the MDOF system and corresponding SDOF system (Calvi and Kingsley 1995).

$$\Delta_{\text{sys}} = \frac{\sum_{i=1}^{n} m_i \Delta_i^2}{\sum_{i=1}^{n} m_i \Delta_i} \tag{1}$$

$$M_{\text{sys}} = \frac{\sum_{i=1}^{n} m_i \Delta_i}{\Delta_{\text{sys}}} \tag{2}$$

   where m_i is the mass associated with the ith location, Δ_i is the target displacement at the ith location and n is the number of lumped mass locations.
3. **Estimate level of equivalent viscous damping.** Utilizing the chosen target displacement for each pier column and estimated yield displacements, the ductility level is calculated for each pier. Yield displacements are estimated from yield curvature. In case of rectangular section yield curvature is obtained from Eq. 3, which is modified slightly from its original form (Priestley et al. 1996) to suitably account low axial load ratio ($P/f_c A_g \leq 0.05$) for tall piers.

$$\phi_y = 1.8 \frac{\varepsilon_y}{h_c} \tag{3}$$

   where ε_y is the reinforcement yield strain, h_c is the depth of the rectangular section. Knowing the displacement ductility demand for each member, the corresponding equivalent viscous damping is estimated by Eq. 4 which is valid for Takeda thin hysteretic rule that generally is suitable for well confined pier section (Priestley et al. 2007). Additional 5% elastic viscous damping (ξ_{el}) is added to the hysteretic damping to account for

[1] With first inelastic mode shape we refer to the first vibration mode of the structure under consideration calculated based on equivalent elastic properties incorporating the material inelasticity and geometric nonlinearity explicitly.

energy dissipation from nonlinearity in the elastic response, soil-structure interaction and other similar mechanisms (Grant et al. 2004).

$$\xi_i = \xi_{\text{el}} + 0.444\left(\frac{\mu_\Delta - 1}{\mu_\Delta \pi}\right) \tag{4}$$

These individual damping values need to be combined in some form to obtain the equivalent SDOF system damping. A weighted average may be computed as given by Eq. 5, where Q_i is the weighting factor. Although various approaches are available in the literature (Kowalsky 2002), the approach based on equal work principle (Dwairi and Kowalsky 2006; Priestley et al. 2007) is followed here.

$$\xi_{\text{sys}} = \sum_{i=1}^{n}\left(\frac{Q_i}{\sum_{k=1}^{n} Q_k}\xi_i\right) \tag{5}$$

$$Q_i = V_i \Delta_i \tag{6}$$

where V_i is shear force associated with ith member, Δ_i is corresponding displacement and n is the total number of energy dissipating elements. Since shear force distribution is unknown at this stage of design procedure, some realistic assumptions should be made to estimate that. The first assumption is: the fraction of total lateral inertia force carried back to the abutments by superstructure bending is **x**. The second one is: all the pier columns are pin-connected with deck in the transverse direction and have geometric cross-section and reinforcement content so that pier base moments are equal. This assumption allows to consider shear forces in piers ($V_{P,i}$) distributed inversely proportional to the pier heights (H_i), assuming all the piers are yielded and have zero post-yield stiffness, as given by Eq. 7. If some piers remain elastic the proportionality coefficient has to be modified by the displacement ductility demand as given by Eq. 8. For abutments behaving elastically, shear forces ($V_{A,i}$) are distributed according to assumed target displacements (Δ_i) so that stiffness requirement remains the same even with unequal displacement demands. Inelastic behaviour of abutments is not considered in this study. A detailed discussion can be found in Priestley et al. (2007).

$$\text{Yielded pier column: } V_{P,I} \propto \frac{1}{H_i} \tag{7}$$

$$\text{Elastic pier column: } V_{P,I} \propto \frac{\mu_{\Delta,i}}{H_i} \tag{8}$$

$$\text{Abutment: } V_{A,I} \propto \Delta_i \tag{9}$$

Combining all the contributions from superstructure damping (ξ_{SS}), abutment damping (ξ_A) and pier damping ($\xi_{P,i}$), the equivalent SDOF system damping is estimated by Eq. 10:

$$\xi_{\text{sys}} = \frac{x\left(\Delta_{\text{sys}} - \Delta_A\right)\xi_{\text{SS}} + x\Delta_A\xi_A + (1-x)\left(\sum_{\text{piers}} Q_{P,i}\xi_{P,i}\right)}{x(\Delta_{\text{sys}} - \Delta_A) + x\Delta_A + (1-x)(\sum_{\text{piers}} Q_{P,i})} \tag{10}$$

where Δ_{sys} is the equivalent SDOF system displacement calculated according to Eq. 1, Δ_A is the average abutment displacement and $Q_{P,i}$ is the ith pier weighting factor given by the relation:

$$Q_{p,i} = \frac{1/H_{P,i}}{\sum_{\text{piers}} 1/H_{P,i}}\Delta_{P,i} \tag{11}$$

Equation 11 is valid only for yielded piers and modified by Eq. 8 for piers those remain elastic during design seismic excitation.

4. **Determine effective period of the equivalent SDOF system.** Utilizing the system target displacement, level of system damping, and elastic response spectra for the chosen seismic demand, the effective period of the equivalent structure is determined as shown in Fig. 1. The design spectrum considered here is a modified Eurocode 8 (CEN 2004) type 1 displacement spectrum for soil type C and peak ground acceleration of 0.5 g, which capped the maximum spectral displacement at time period $T_D = 4.0s$ instead of 2.0s (Priestley et al. 2007). The scaling of design spectrum due to various values of viscous damping is done using Eq. 12.

$$\Delta_\xi = \Delta_5 \left(\frac{10}{5+\xi}\right)^{0.5} \tag{12}$$

Once the effective time period (T_{sys}) has been determined, the effective stiffness (K_{sys}) and design base shear (V_B) are computed by Eqs. 13 and 14, respectively.

$$K_{\text{sys}} = M_{\text{sys}} \left(\frac{2\pi}{T_{\text{sys}}}\right)^2 \tag{13}$$

$$V_B = K_{\text{sys}} \Delta_{\text{sys}} \tag{14}$$

5. **Distribution of lateral inertia loading.** This step involves distribution of design base shear as inertia forces to the masses of the original MDOF structure in accordance with the assumed target displacement profile by using Eq. 15.

$$F_i = V_B \frac{m_i \Delta_i}{\sum_{i=1}^{n} m_i \Delta_i} \tag{15}$$

6. **Estimate design strength required at critical locations.** In order to estimate design strength at critical locations, a linear static analysis is performed using the load vector computed at step 5 (Eq. 15). As a matter of necessity, analytical model used for the static analysis should represent appropriate stiffness distribution across the bridge under consideration. For example, elements designed to be remain elastic under design earthquake are represented by elastic stiffness (or secant stiffness to the yield displacement) whilst yielded elements are modeled by secant stiffness to their respective target displacement as computed by Eq. 16

$$(K_{\text{eff}})_i = \frac{V_i}{\Delta_i} \tag{16}$$

where Δ_i and V_i are the displacement achieved and base shear carried by the piers. Since the design process started with two assumptions, namely displacement shape of the bridge and distribution of seismic base shear among different members, it is now time to verify those. If the assumed quantities match well with the computed ones (obtained from the elastic analysis), the design process completes. Otherwise, the same procedure will be repeated until the convergence achieves. Each new iteration starts with the values computed at the previous step. This iterative process was first proposed by Priestley and Calvi (2003).

7. **Design the MDOF structure.** In this step, the critical sections are designed for forces estimated in the previous step and detailed to provide necessary displacement capacity. For example, at the pier base, longitudinal reinforcements are provided to achieve the design strength required from the previous step and transverse reinforcements are

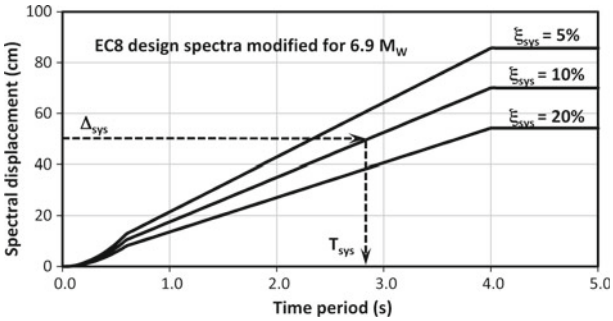

Fig. 1 Effective period calculation based on DDBD procedure

provided to achieve the curvature demand imposed by the design ground motion by employing the following Eq. 17.

$$\phi_{\text{req}} = \frac{M_{\text{design}}}{E_c I_{\text{sec}}} \tag{17}$$

where, ϕ_{req} is the required curvature, M_{design} is the design moment at that section excluding the P-Δ effect (if any), E_c is the short-term modulus of elasticity of concrete and I_{sec} is the secant moment of inertia of the section derived from the secant stiffness K_{eff}.

3 Issues related to long span bridges and corresponding modifications

A straightforward extension of the above mentioned procedure is, however, not possible for long span bridges because of the following reasons.

3.1 Irregular distribution of flexural strengths among piers

First, while estimating the system damping it is assumed that flexural strength for all pier sections at base are same, thus total base shear force is distributed in proportion to the inverse of respective pier heights (Eqs. 7 and 8). This is not true for long span bridges where span lengths as well as pier heights are often varying significantly and it causes a substantial amount of variation in flexural strength demands at pier bases. Moreover, the design of piers for this category of bridges is often governed by different load combinations other than that required from seismic load combination. Thus it is not always possible to provide same flexural strength at all pier bases. Nonetheless, the same philosophy as well as equations can be used for this category of bridges but with a modification in the original formulation. In this study, a factor (α) is introduced in Eqs. 7 and 8 which represents the ratio of flexural strength of a pier to the flexural strength of the critical pier. Once this factor is obtained either from other load combinations or from engineering judgment, shear force distribution can be determined from the Eqs. 18 and 19.

$$V_{P,I} \propto \frac{\alpha_{P,i}}{H_{P,i}} \quad \text{(Ductile column)} \tag{18}$$

$$V_{P,I} \propto \frac{\alpha_{P,i}\mu_{P,i}}{H_{P,i}} \quad \text{(Elastic column)} \tag{19}$$

3.2 Incorporation of influence of massive tall piers

Second, the secant stiffness of pier element estimated using Eq. 16 is derived from the assumption that inertia force is applied at the pier top only. It is valid for short-to-moderate span bridges, where a certain percentage of pier mass (generally 1/3rd of the total mass) along with tributary deck mass is lumped at the pier top and the rest of the pier is assumed as mass-less (Priestley et al. 1996). However, this assumption may lead to a serious underestimation of total base shear for massive tall piers, which are generally common for long span bridges. This is exemplified further in the following paragraph.

Consider a simple bridge system having a span arrangement of 60-100-60 m with pier height of 50 m. The total weight of one pier column is equal to 31 MN whereas tributary deck weight on that pier is 29.7 MN. When 1/3rd of pier weight is lumped at top, the total weight for seismic base shear calculation is ~40 MN which is ~35% less than the actual seismic weight (60.7 MN). This underestimation of base shear will increase further for bridges with taller and massive piers. To avoid this underestimation, a proposal is made based on the principles of statics. The pier element is discretized into a number of sub-elements and tributary masses are lumped at each intermediate node. Since displacement at pier top and lateral force distribution at any stage of DDBD are known, the secant stiffness corresponding to displacement at pier top can be calculated from Eq. 22. The derivation of Eq. 22 is as follows.

Consider a simple cantilever beam under a lateral force vector as shown in Fig. 2, which represents the condition of pier under inertia loading from design ground motion. The height-wise distribution and magnitude of lateral force vector are known from Eq. 15 mentioned above. However, the exact magnitude of lateral force at pier top (F_N) is unknown since it depends also on the tributary deck weight which is difficult to estimate when deck is discretized into a number of sub-elements and masses are lumped at the nodes. So, an indirect procedure is followed here to estimate the lateral force at pier top. Since the total shear at each pier base and lateral forces along the pier height are known, the only unknown parameter, i.e., effective lateral force at pier top, can be estimated using the Eq. 20.

$$F_N = V_B - \sum_{i=1}^{N-1} F_i \tag{20}$$

When the lateral force vector imposed on the pier is known, the displacement at the pier top can be determined using the basic principles of statics as shown in Eq. 21.

$$\Delta_{\text{top}} = \sum_{i=1}^{N} \Delta_i = \sum_{i=1}^{N} \frac{\frac{1}{2} F_i h_i \left(H - \frac{h_i}{3}\right)}{E_c I_{\text{sec}}} = \frac{\left(V_B - \sum_{i=1}^{N-1} F_i\right) \frac{H^3}{3} + \sum_{i=1}^{N-1} \frac{1}{2} F_i h_i \left(H - \frac{h_i}{3}\right)}{E_c I_{\text{sec}}} \tag{21}$$

Rearranging Eq. 21, the secant stiffness at pier base is estimated form Eq. 22.

$$E_c I_{\text{sec}} \Delta_{\text{top}} = \left(V_B - \sum_{i=1}^{N-1} F_i\right) \frac{H^3}{3} + \sum_{i=1}^{N-1} \frac{F_i h_i^2}{2} \left(H - \frac{h_i}{3}\right) \tag{22}$$

where, V_B and H are the base shear and overall height of the pier under consideration, respectively, F_i is the inertia force related to the tributary mass lumped at ith intermediate node, h_i is the height of application of the inertia force from pier base, E_c is the short term modulus

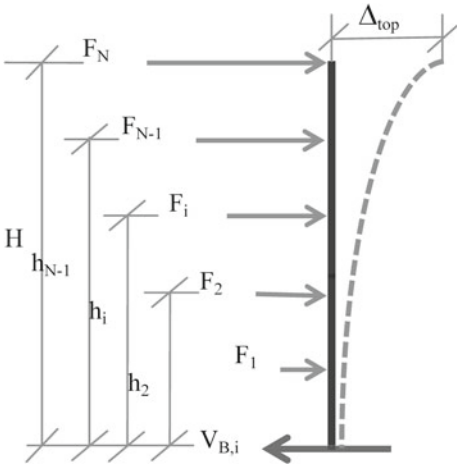

Fig. 2 Displaced shape of a pier under lateral force vector

of elasticity for concrete, I_{sec} is the secant moment of inertia of the pier section at base and Δ_{top} is the design displacement at pier top.

3.3 Inclusion of higher mode effects on flexural strength of plastic hinges

The third novelty of this procedure is the use of modal superposition principle for determining the flexural strength demand at potential plastic hinge locations. In previous studies (Alvarez Botero 2004; Ortiz Restrepo 2006; and Priestley et al. 2007), higher mode effects were considered only for determining the design elastic responses (e.g. transverse moment at deck, abutment shear force etc.), whereas inelastic responses, such as flexural strengths at plastic hinge locations, were taken directly from the first inelastic mode. This is justified by the fact that mass participation factor for the first inelastic mode was always more than 80% for the bridges considered in their study. However, this assumption is not applicable to long span bridges because of inherent flexibility. In fact, for some bridges used in this study, the estimated mass participation factor for the first inelastic mode is as low as 32% only. Thus higher mode effects are necessary to be incorporated in the DDBD procedure even for estimating flexural strengths also; otherwise it may lead to a serious underestimation of actual strength demand.

In his study, Ortiz Restrepo (2006) evaluated four different elastic modal superposition procedures and concluded that the Effective Modal Superposition (EMS) procedure always provides conservative envelope for deck transverse moment and abutment shear. Priestley et al. (2007), in a subsequent publication, also supported the use of EMS procedure for bridge design. Following their suggestion, the EMS procedure is adopted here with a modification. As defined in its original formulation, the EMS procedure, which is fully compatible with the substitute structure philosophy, uses a Response Spectrum Analysis (RSA) after completion of the DDBD procedure, whereby stiffnesses of members having plastic hinges (e.g., piers) are represented by secant stiffnesses to the peak displacement response, while elastic members (e.g., superstructure and abutment) are modelled by initial-stiffness values; and seismic hazard is defined by a 5% damped elastic design spectrum. The final results are obtained combining the higher-mode elastic forces from such analysis with the DDBD inelastic first-mode design forces using appropriate combination rules (SRSS or CQC). In this study, two different design spectra are instead used to determine the design responses at critical locations

Table 1 Salient features of the bridges used in this study

Bridge No.	Span arrangement and Pier heights (m)	Average geometric properties of deck	Cross-section details of piers
B1	Span : 60-100-60	$A = 9.96\,\text{m}^2$	Width : 4.0 m
	Pier : 50-50	$I_Y = 35.93\,\text{m}^4$	Depth : 7.0 m
		$I_Z = 77.02\,\text{m}^4$	Thickness : 1.2 m
B2	Span : 80-160-20-240-20-140	$A = 19.26\,\text{m}^2$	Width : 4.5 m
	Pier : 40-80-80-80-80	$I_Y = 297.44\,\text{m}^4$	Depth : 10.3 m
		$I_Z = 647.40\,\text{m}^4$	Thickness : 1.0 m
B3	Span : 40-100-180-100-40	$A = 13.67\,\text{m}^2$	Width : 3.0 m; 10.9 m
	Pier : 20-100-100-20	$I_Y = 150.36\,\text{m}^4$	Depth : 7.7 m; 12.5 m
		$I_Z = 189.03\,\text{m}^4$	Thickness : 0.5 m; 1.0 m
B4	Span : 60-100-120-100-60	$A = 9.96\,\text{m}^2$	Width : 4.0 m
	Pier : 50-50-50-50	$I_Y = 35.93\,\text{m}^4$	Depth : 7.0 m
		$I_Z = 77.02\,\text{m}^4$	Thickness : 1.2 m
B5	Span : 60-100-60-100-120	$A = 9.96\,\text{m}^2$	Width : 4.0 m
	Pier : 50-50-50-50	$I_Y = 35.93\,\text{m}^4$	Depth : 7.0 m
		$I_Z = 77.02\,\text{m}^4$	Thickness : 1.2 m
B6	Dimensions are same as B4 but one movement joint has been introduced at 120 m span, 40 m away from the pier P2		
B7	Dimensions are same as B5 but one movement joint has been introduced at 60 m span, 30 m away from the pier P2.		

as a combination of all modes by SRSS or CQC rule: 5% damped design spectrum is used for determining the design elastic responses, such as deck transverse moment and consequent abutment shear, whereas damped design spectrum, with damping value equals to the system damping obtained from the DDBD procedure, is used for combining the inelastic responses, such as flexural strength demand at the plastic hinge locations. In this way, it is expected to obtain more realistic design values for both elastic and inelastic responses when higher mode contributes significantly to the final design responses. The whole procedure is exemplified further in Appendix.

4 Verification study

Accuracy of the proposed modifications, as described in the previous section, has been evaluated through rigorous nonlinear Response History Analyses (RHA) of seven long span bridges reproducing real existing bridge geometry and thus incorporates realistic distribution of mass and stiffness along the bridge length in the current evaluation procedure. Salient features of each bridge are presented in Table 1 and in Fig. 3. Four real accelerograms have been selected and scaled to match the design spectrum used in the DDBD procedure from 2s to 4s time period range as all the bridges have secant period that falls within that range, while two records have been generated using the SIMQKE program (Gasparini and Vanmarcke 1976) so that a balance between real and artificial accelerograms can be achieved. The peak ground acceleration of selected records are varying from 0.36 g to 1.10 g and have

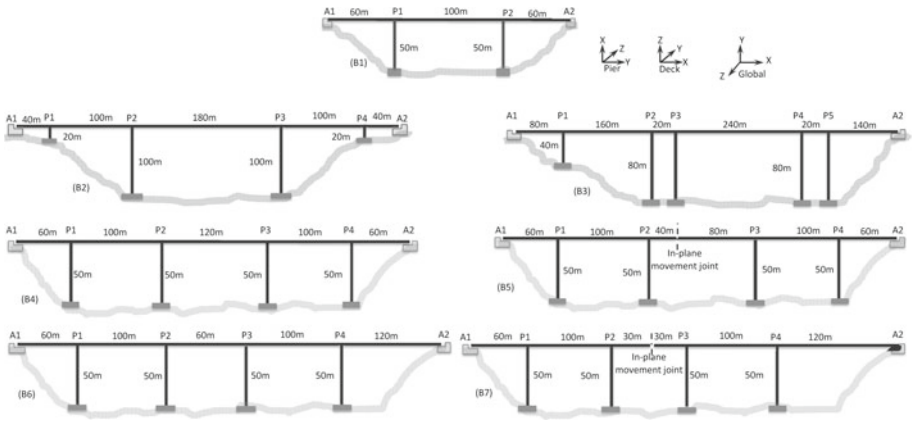

Fig. 3 Schematic diagram of the bridges used in this study (drawn not to scale)

duration varying from 20s to 120s. Thus it is expected that mean responses obtained from RHA analyses using these acceleration records would capture the variability introduced by the ground motion records.

In the verification process, a bridge is analysed according to the modified DDBD procedure (named *mDDBD* in the figures), the original DDBD procedure (named *DDBD* in the figures) and the current force based design (named *FBD* in the figures) procedure independently and detailed with the reinforcement required from each procedure. The current Eurocode 8 (CEN 2005) recommendation is followed here with a behaviour factor equals to 1.0, as suggested for limited ductile piers, when the bridges are designed according to the FBD procedure. Each of the seven bridges designed according to different procedures (and hence detailed with different reinforcement ratios in agreement with Fig. 4) was subjected to a suit of six ground motions as described earlier. The mean responses obtained from RHA are then compared with the designed responses. All the analyses have been carried out using the freely available software OpenSees (2006). Details of mathematical models and analysis parameters adopted for this study can be found elsewhere (Adhikari 2007).

Two response parameters—transverse deck displacement and moment profile—along with reinforcement content (in % of gross area) at pier base obtained from different design procedures are compared in the following figures (Figs. 4, 5, 6, 7, 8). Based on those figures following observations can be made.

1. Higher modes have, indeed, influence on both elastic and inelastic responses of a bridge, in contrast with the earlier studies where it was assumed that higher modes influenced only the elastic responses. This influence is distinctly visible from Fig. 4, whereby longitudinal reinforcement content (in % of gross area) which governs the inelastic responses at pier base is varied significantly for some piers when higher modes are considered, e.g., pier P1 of bridge 2 and pier P1 and P4 of bridge 3, while others are not influenced so much. It is also observed that this influence diminishes with increase in inelastic deformation demand.
2. In the analysed cases, the reinforcement content obtained from any form of DDBD is generally much less than that obtained from FBD procedure (Fig. 4). Thus it can be inferred that the DDBD procedure provides a more economical design procedure than the current FBD procedure. This inference is reinforced further when deck transverse displacement profiles (Fig. 7) and moment (Fig. 8) obtained from different design

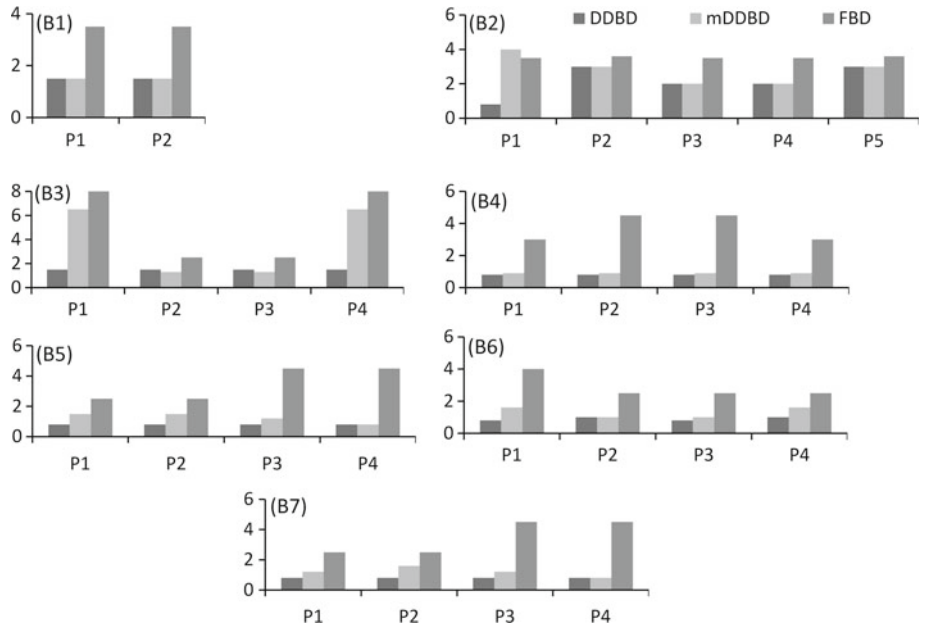

Fig. 4 Reinforcement content (in % of gross sectional area) at pier base obtained from three different design philosophies: original DDBD, modified DDBD and FBD

procedures are compared with the mean response obtained from RHA. It is observed that FBD procedure always underestimates significantly the deck displacement and overestimates the deck moment compared to those obtained from mean value of RHA. This FBD failure to predict the correct response of the structure may lie in the use of non appropriate design pier member stiffness. Indeed, since the bridges studied here fall within the category of limited ductile system, applying the force based design procedure gross sectional stiffness is used and behaviour factor is assumed equal to 1.0: this implies that the bridges are expected to behave elastically, in contrast with the time history results (Fig. 7).

3. As observed from Fig. 5, deck displacement profiles obtained from modified version of DDBD are in close agreement with that obtained from the mean of six RHA, except in one case—pier 3 of bridge 6—where modified DDBD underestimates the response of pier top. However, this can be explained as follows. While bridge 6 was designed according to the DDBD procedure, the above mentioned pier remain elastic under the design level earthquake (as the yield and target displacement are same); but the amount of reinforcement provided at the pier base was determined by employing a design spectrum that was scaled down as per system damping which was obviously higher than 5.0% as used for elastic elements. Thus the reinforcement provided at the pier base was less than that actually required for elastic behaviour of pier column and that caused a higher displacement at pier top during RHA. In Fig. 5 deck displacement profiles obtained from original and modified version of DDBD are also compared. It is interesting to notice that for flexible bridges, such as bridge no 4 to bridge no 7, the increase in reinforcement is not so significant as the modification of displacement profile when higher modes are considered.

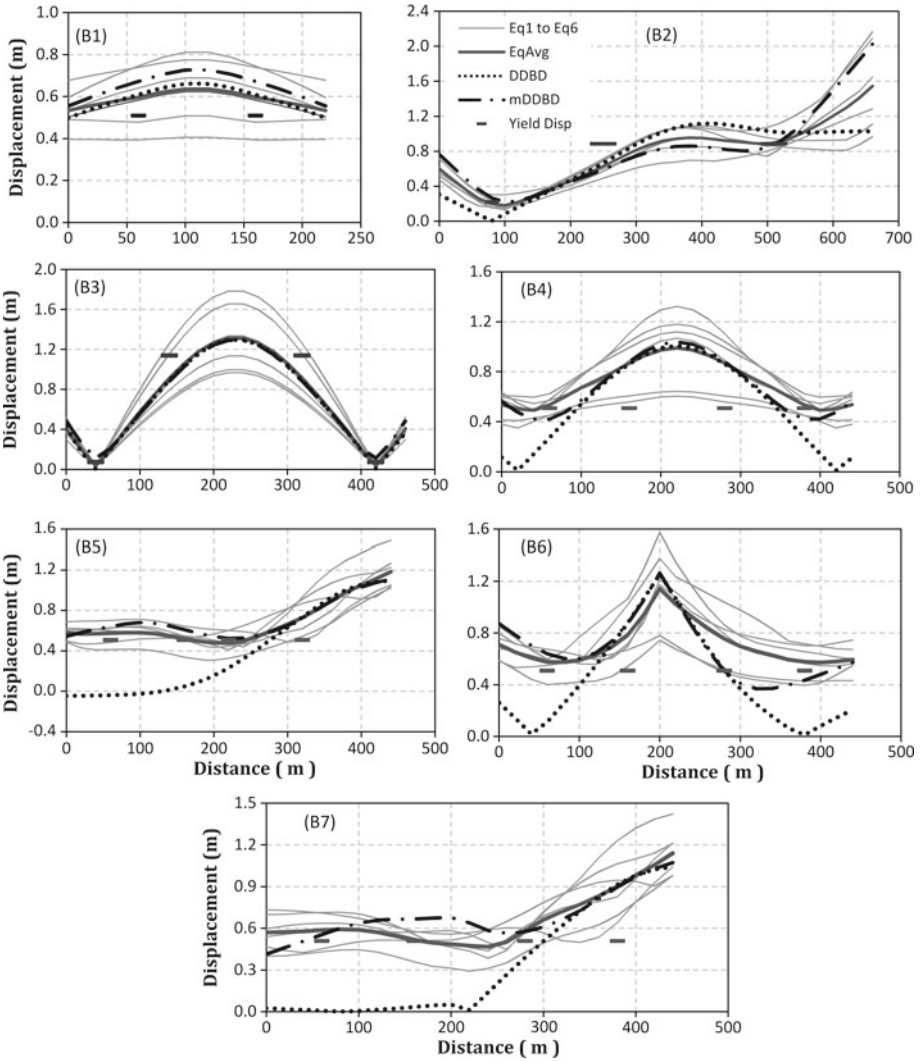

Fig. 5 Comparison of deck transverse displacements (representative of inelastic response) obtained from original DDBD, modified DDBD and nonlinear dynamic analyses

4. When transverse deck moment is compared for different bridges obtained from modified DDBD procedure (Fig. 6), a close agreement is observed for most of the cases except for bridge 7. However, this is not so important issue as the transverse capacity of deck is often provided sufficiently higher than that required from seismic load combination.

5 Conclusion

Described in this paper is a study aimed at identifying the potential limitations and subsequent modifications, if required, of the current DDBD procedure for long span concrete bridges

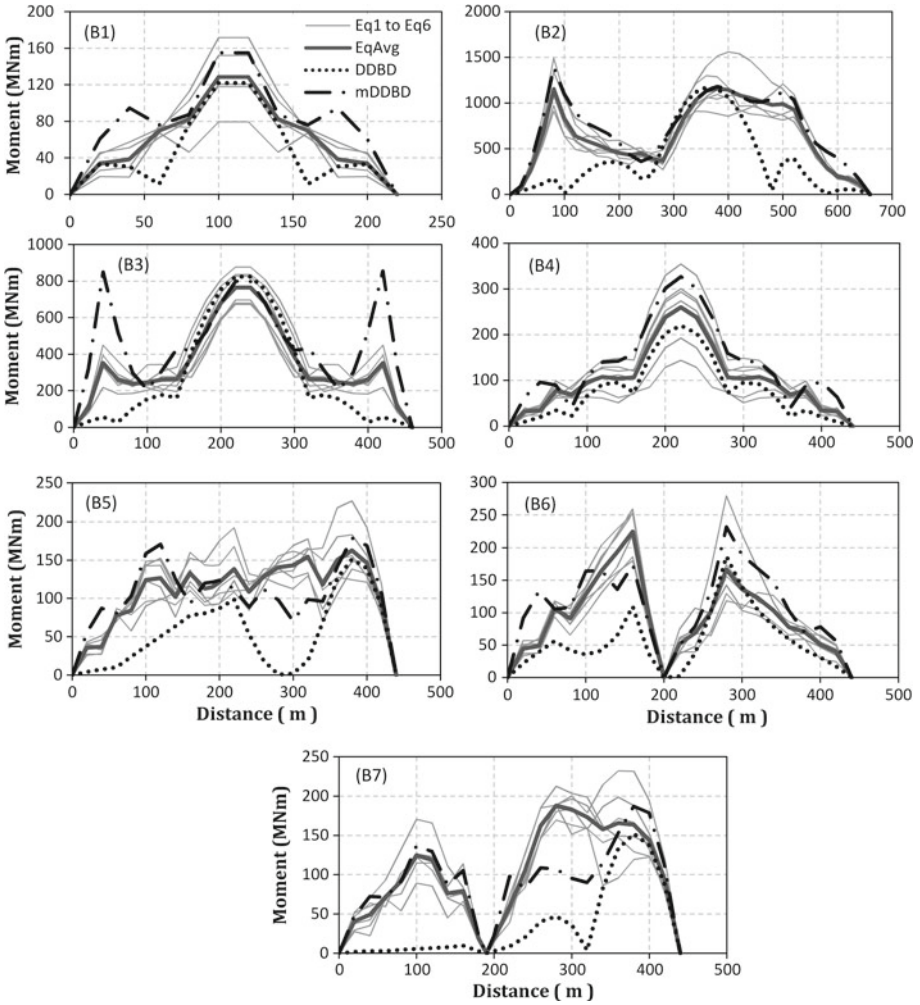

Fig. 6 Comparison of deck transverse moment (representative of elastic response) obtained from original DDBD, modified DDBD and nonlinear dynamic analyses

under transverse excitation. Three fundamental modifications are proposed here, namely, the distribution of base shear across the piers and abutments when piers have different moment carrying capacity instead of considering equal strength, consideration of lumped masses along the pier height which is useful for tall massive piers and modal superposition for determining the design inelastic responses also. With these modifications, designers now have more freedom for assigning flexural strengths among the piers and corresponding distribution of shear forces apart from the more economical solution than the current FBD procedure mentioned in the Eurocode 8 (CEN 2004).

Acknowledgments Part of this work has been carried out under the financial auspices of "Reluis (Rete dei Laboratori Universitari di Ingegneria Sismica) through the project, Progetto esecutivo 2005–2008 (Attuazione Accordo di Programma Quadro DPC-Reluis del 15-03-2005)–Linea 4, "Sviluppo di approcci agli spostamenti per il progetto e la valutazione della vulnerabilità". Such support is gratefully acknowledged by the authors. The authors would like to acknowledge Prof. Nigel Priestley for the useful discussions on the subject.

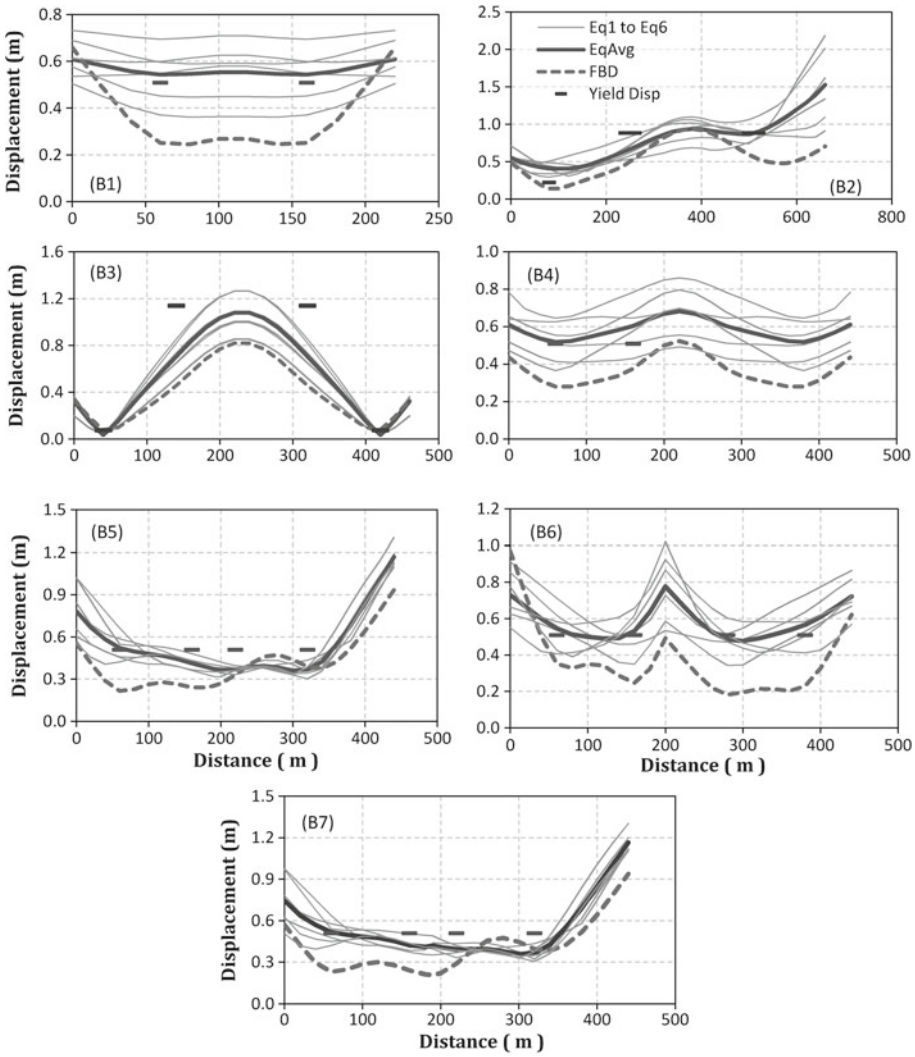

Fig. 7 Comparison of deck transverse displacements (representative of inelastic response) obtained from FBD and nonlinear dynamic analyses

Appendix: Sample calculation for one bridge

A sample calculation of DDBD procedure for Bridge No 1, as shown in Fig. 3 (B1), having average sectional properties tabulated in Table 1 is presented below.

Step 1 Assumptions

A half-sine based displacement shape is assigned for transverse deck movement considering abutment stiffness $K_A = 5000\,\text{kN/m}$ and overall span length $L = 220\,\text{m}$ ignoring the influence of piers (Alvarez Botero 2004). Piers are assumed to be displaced in linear profile. The ordinates of displacement shape of bridge deck and of each pier, calculated at the nodal points

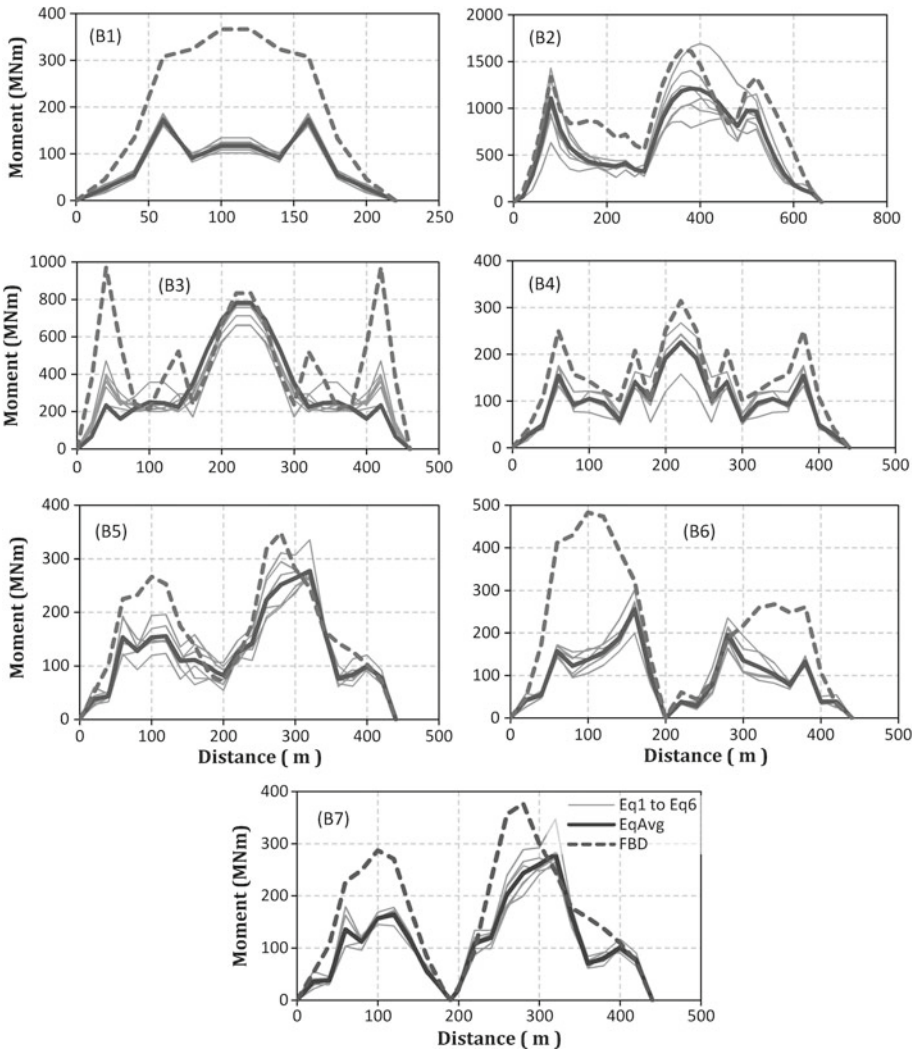

Fig. 8 Comparison of deck transverse moment (representative of elastic response) obtained from FBD and nonlinear dynamic analyses

where tributary masses are lumped, are presented in Tables 2 and 3; and shown graphically in Fig. 9. The displacement shape $\phi(x)$ of deck as a function of x from the left abutment is given by

$$\phi(x) = \frac{\sin(\pi x/L) + \pi^3 B}{1 + \pi^3 B} = \frac{\sin(0.01428x) + 1.3826}{2.3826}$$

where constant B is defined as

$$B = \frac{\mathrm{EI}}{K_A L^3} = \frac{30 \times 10^6 \times 77.02}{5000 \times 220^3} = 0.04459$$

Table 2 Initial transverse displaced shape of the bridge deck

Distance (m) of the node on the deck from the left abutment (A1)											
0	20	40	60	80	100	120	140	160	180	200	220
0.580	0.699	0.807	0.897	0.962	0.996	0.996	0.962	0.897	0.807	0.699	0.580

Table 3 Initial transverse displaced shape of each pier

Distance (m) of the node on the pier from the base					
0	10	20	30	40	50
0.000	0.179	0.359	0.538	0.718	0.897

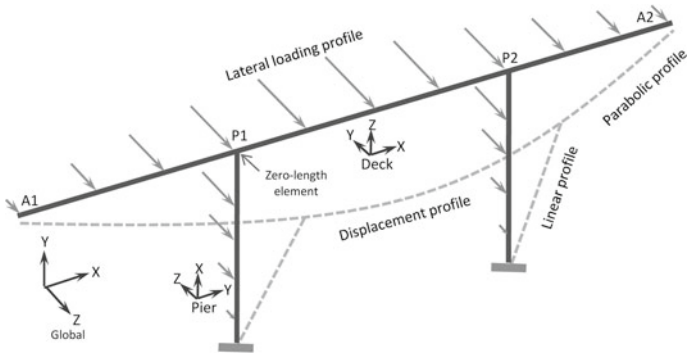

Fig. 9 Initial displacement profile of the bridge

Table 4 Target displacement of the bridge deck in transverse direction

Distance (m) of the node on the deck from the left abutment (A1)											
0	20	40	60	80	100	120	140	160	180	200	220
1.132	1.362	1.574	1.750	1.876	1.942	1.942	1.876	1.750	1.574	1.362	1.132

It is also assumed that 25% of total seismic base shear will be transferred to the ground by elastic bending of deck and abutments; i.e., $x = 0.25$.

Step 2 Define target displacement profile of the bridge

The displacement shape obtained in Step 1 is scaled in such a fashion that at least one column reaches its displacement capacity which is computed by limiting its ultimate drift ratio to 3.5%. Therefore, target displacement of each pier at deck level is $\Delta_m = 0.035 \times 50\,\text{m} = 1.75\,\text{m}$. Accordingly, displacement profile of the whole bridge is scaled and presented in Tables 4 and 5.

Table 5 Target displacement of each pier in transverse direction

Distance (m) of the node on the pier from the base					
0	10	20	30	40	50
0.000	0.350	0.700	1.050	1.400	1.750

Table 6 Inertial weight (kN) associated with each deck node for transverse movement

Distance (m) of the node on the deck from the left abutment (A1)											
0	20	40	60	80	100	120	140	160	180	200	220
3300	6600	6600	9700	6600	6600	6600	6600	9700	6600	6600	3300

Table 7 Inertial weight (kN) associated with each pier node for transverse movement

Distance (m) of the node on the pier from the base					
0	10	20	30	40	50
0.000	6200	6200	6200	6200	9700

Step 3 Determine properties of equivalent SDOF system

Inertia weights lumped at each deck and pier nodes associated with the transverse bridge movement are presented in Tables 6 and 7. These weights include self weight of superstructure (330 kN/m) and substructure (620 kN/m), respectively, for deck and pier nodes.

Step 3a Determination of equivalent SDOF system displacement and mass

Displacement capacity of equivalent SDOF system when bridge reaches its design displacement profile is given by $\Delta_{sys} = 1.534$ m (Eq. 1).
The effective mass is computed as $m_{sys} = 11565$ Mt (88.33% of total transverse mass) from Eq. 2.

Step 3b Determination of equivalent viscous damping ratio for all elements

In order to determine equivalent viscous damping ratio, it is necessary to know the ductility of all elements transferring seismic force. Ductility of deck is taken as 1.0 because of its elastic nature. In case of pier columns, yield curvature is computed by Eq. 3.

$$\phi_y = 1.8\frac{0.002375}{7.0}\,\mathrm{m}^{-1} = 6.11 \times 10^{-4}\,\mathrm{m}^{-1}$$

where yield strain of reinforcement is 0.002375 m/m and depth of pier section is 7.0 m.

The overall height of each pier including strain penetration at base is $H = 50 + 0.022 \times 475 \times 0.04$ m $= 50.418$ m for 40 mm diameter of longitudinal reinforcements of expected yield strength 475 MPa.

$$\text{Yield displacement at pier top } \Delta_y = 6.11 \times 10^{-4} \times \frac{50.418^2}{3} m = 0.509\,\text{m}$$

$$\text{And available ductility capacity } \mu_\Delta = \frac{1.750}{0.509} = 3.438$$

Thus equivalent viscous damping ratio for each pier

$$\xi_p = 0.05 + 0.444 \times \left(\frac{3.439 - 1}{3.439\pi}\right) = 15.02\% \text{ of critical damping.}$$

Step 3c Determination of base shear distribution among different elements

The equivalent viscous damping ratio depends also on the base shear distribution among all elements transferring seismic force. The base shear distribution is calculated under the assumption that yield moment capacity of all pier sections at base is same. Thus shear force carried by individual pier is inversely proportional to their height, provided all the piers are yielded under the design earthquake.

$$V_{P,1} = V_{P,2} = (1 - x)\frac{1/H_{1(2)}}{1/H_1 + 1/H_2} V_B = (1 - 0.25)\frac{1/50}{1/50 + 1/50} V_B = 0.375 V_B$$

where $V_{P,1}$, $V_{P,2}$ and H_1, H_2 are base shear carried by and heights of 1st and 2nd pier, respectively, and V_B is the total base shear.

Step 3d Determination of equivalent system damping

For the sake of simplicity, it is assumed that abutment and deck damping is the same. Thus from Eq. 10, the equivalent system damping can be estimated as follows

$$\xi_{\text{sys}} = \frac{0.25 \times 1.132 \times 5.00 + (1 - 0.25) \times \left(\frac{2\times 1.750 \times 15.02}{50}\right) \Big/ \frac{2}{50}}{0.25 \times 1.132 + (1 - 0.25) \times \left(\frac{2\times 1.750}{50}\right) \Big/ \frac{2}{50}} = 12.76\%$$

Step 3e Determination of design base shear

Utilizing the design spectrum previously defined (Fig. 1), damped by the equivalent system damping according to Eq. 12, and the value of system displacement, it is observed that maximum possible displacement demand is 0.857 m which is much lower than the computed one. This implies structure might remain elastic under design earthquake: it may often happen when the bridge has tall and hence very flexible piers. Accordingly, displacement profile of the bridge is modified by reducing the target displacement demand and keeping the same shape so that equivalent system displacement reaches the maximum displacement at appropriate damping value. The revised displacement is presented in Tables 8 and 9.

Following the same procedure, properties of equivalent SDOF system are obtained as follows.

$$\Delta_{\text{sys}} = 0.720\,\text{m} \quad \text{and} \quad \xi_{\text{sys}} = 9.16\% \text{ of critical damping}$$

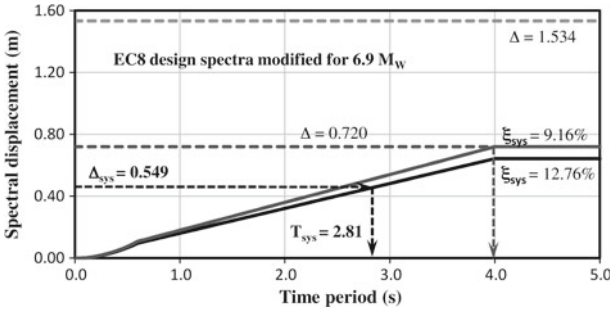

Fig. 10 Computation of effective period

Table 8 Revised transverse displacement profile of the deck

Distance (m) of the node on the deck from the left abutment (A1)											
0	20	40	60	80	100	120	140	160	180	200	220
0.531	0.640	0.739	0.822	0.881	0.912	0.912	0.881	0.822	0.739	0.640	0.531

Table 9 Revised transverse displacement profile of each pier

Distance (m) of the node on the pier from the base					
0	10	20	30	40	50
0.000	0.164	0.329	0.493	0.657	0.822

Table 10 Transverse inertia force (kN) applied at deck nodes

Distance (m) of the node on the deck from the left abutment (A1)											
0	20	40	60	80	100	120	140	160	180	200	220
441	1062	1227	2005	1463	1514	1514	1463	2005	1227	1062	441

Utilizing these values along with the design spectrum (Fig. 10), secant period of the equivalent SDOF system is $T_{\text{sec}} = 4.0\,\text{s}$ and corresponding secant stiffness is

$$K_{\text{sys}} = \frac{4\pi^2 \times 11565}{4.0^2} = 28535\,\text{kN/m}$$

Therefore, seismic base shear is equal to $V_b = 28535 \times 0.720 = 20550\,\text{kN}$ (Eq. 14) and it is distributed among different inertia mass locations using Eq. 15 (Tables 10, 11). Note that, the P-Delta effect on pier columns are reduced by limiting the secant period to 4.0 s; if P-Delta effect is not critical, then higher secant period can be used.

Step 4 Determination of effective member stiffness

Members behaving elastically under design earthquake are represented by their elastic stiffness (or secant stiffness to yield displacement). Examples are deck slab and abutments. In case piers, the effective stiffness is computed using Eq. 22, where base shear is computed by

Table 11 Transverse inertia force (kN) applied at pier nodes

Distance (m) of the node on the pier from the base					
0	10	20	30	40	50
0.000	256	513	769	1025	2005

Table 12 Computed displacement profile (m) of bridge deck

Distance (m) of the node on the deck from the left abutment (A1)											
0	20	40	60	80	100	120	140	160	180	200	220
0.564 (0.531)	0.647 (0.640)	0.722 (0.739)	0.785 (0.822)	0.834 (0.881)	0.862 (0.912)	0.862 (0.912)	0.834 (0.881)	0.785 (0.822)	0.722 (0.739)	0.647 (0.640)	0.564 (0.531)

In parenthesis are reported the results of the previous calculation

Table 13 Computed displacement profile (m) of each pier

Distance (m) of the node on the pier from the base					
0	10	20	30	40	50
0.000 (0.000)	0.046 (0.164)	0.169 (0.329)	0.347 (0.493)	0.558 (0.657)	0.785 (0.822)

In parenthesis are reported the results of the previous calculation

$$V_{P,i} = (1 - 0.25) \times 20550 \times \frac{1/50}{1/50 + 1/50} = 7706\,\text{kN}$$

and lateral force at pier top is $F_N = 7706 - (1025 + 769 + 513 + 256) = 5143\,\text{kN}$

Therefore, secant stiffness at pier base is given by

$$EI_{\text{sec}}\Delta_{top} = 5143\frac{50^3}{3} + 1025\frac{40^2}{2}\left(50 - \frac{40}{3}\right) + 769\frac{30^2}{2}\left(50 - \frac{30}{3}\right) + 513\frac{20^2}{2}\left(50 - \frac{20}{3}\right) + 256\frac{10^2}{2}\left(50 - \frac{30}{3}\right) = 263243667\,\text{kNm}^3$$

Now plugging the values of elastic modulus of concrete ($E = 30822\,\text{MPa}$) and displacement at pier top ($\Delta_{\text{top}} = 0.822\,\text{m}$) into the above relation, the secant moment of inertia at pier base is $I_{\text{sec}} = 10.39\,\text{m}^4$.

Step 5 Perform linear static analysis of the structure

Knowing the values of element stiffness (Step 4) and lateral load vector (Step 3e), it is now possible to perform a linear elastic static analysis of the structure to check the assumptions made at the beginning and to find design strengths at the critical locations. The computed displacements profile and distribution of base shear are tabulated in Tables 12, 13 and 14.

The calculated fraction of load carried by the abutments is 0.27 (compared with initial assumption of 0.25) and system displacement is estimated as 0.70 m (compared with target system displacement of 0.72 m). Since both the assumptions are quite close to the calculated values, the analysis is stopped here. Columns are designed for the base moment

Table 14 Computed base shear at abutments and piers

A1	P1	P2	A2
2821 (2569)	7454 (7706)	7453 (7706)	2821 (2569)

In parenthesis are reported the results of the previous calculation

Table 15 Computed displacement profile (m) of the bridge deck

Distance (m) of the node on the deck from the left abutment (A1)											
0	20	40	60	80	100	120	140	160	180	200	220
0.497 (0.488)	0.539 (0.534)	0.575 (0.575)	0.608 (0.611)	0.639 (0.644)	0.659 (0.665)	0.659 (0.665)	0.639 (0.644)	0.608 (0.611)	0.575 (0.575)	0.539 (0.534)	0.497 (0.488)

Table 16 Computed displacement profile (m) of each pier

Distance (m) of the node on the pier from the base					
0	10	20	30	40	50
0.000 (0.000)	0.035 (0.035)	0.129 (0.130)	0.266 (0.267)	0.431(0.433)	0.608 (0.611)

Table 17 Computed base shear (kN) at abutments and piers

A1	P1	P2	A2
2485 (2434)	12265 (12316)	12265 (12316)	2485 (2434)

of $M_{\text{design}} = 338\,\text{MNm}$ obtained from the analysis and corresponding curvature demand estimated from Eq. 17.

$$\phi_{\text{req}} = \frac{338}{30822 \times 10.39}\text{rad/m} = 0.001055\,\text{rad/m}$$

From moment-curvature analysis of the column section, it is found that 0.4% reinforcement is sufficient to achieve that target curvature under the design moment. However, this reinforcement demand is much lower than that required from other considerations (such as gravity loading, wind loading etc). When higher reinforcement (say 1.20% in this case) is provided to suit other requirements, the pier columns become stiffer and thus attract higher seismic forces. Therefore further analysis is performed by reducing again the target displacement of the system so that moment demand at pier base reaches its capacity. The final converged displaced shape is presented in Tables 15 and 16 whilst base shear demand is tabulated in Table 17. The values in the bracket are the starting point for the last converged step.

The calculated fraction of load carried by the abutment is 0.17 (compared with the assumption of 0.17) and system displacement is estimated as 0.548 m (compared with target system displacement of 0.549 m). In order to incorporate the effects of higher modes of vibration, two modal analyses are performed using secant stiffness of all elements obtained at the last step of DDBD iteration—one with 5% damped spectrum for elastic responses such as abutment shear forces, transverse deck moment; and the other with 7% damped (system damping) spectrum for ductile responses, such as deck displacement and flexural moment capacity at

pier bases. Responses from different modes are combined by standard Square Root of Sum of Squares (SRSS). The new displaced shape is shown in Fig. 5.

The new design moment at pier base is 566 MNm and corresponding curvature demand is 0.00075 rad/m. This flexural demand can be achieved by providing 1.2% longitudinal reinforcement which is matched with the requirement from other considerations.

Step 6 Check for P-Δ effects

$$\text{The stability index } \theta_A = \frac{P\Delta_{\max}}{M_{\text{base}}} = \frac{60.10 \times 0.611}{565.81} = 0.065 < 0.10$$

As this is less than 0.10, P-Δ effects can be ignored as recommended by Priestley et al. (2007).

Finally, other elements of the bridge are detailed following the capacity design principle in order to prevent any sort of brittle failure.

References

Adhikari G (2007) Direct displacement based design: long span bridges with/without in-plane movement joint. Masters dissertation, European school for advanced studies in reduction of seismic risk (ROSE School), University of Pavia, Italy

Alvarez Botero JC (2004) Displacement-based design of continuous concrete bridges under transverse seismic excitation. Masters dissertation, European school for advanced studies in reduction of seismic risk (ROSE School), University of Pavia, Italy

Aschheim MA, Black EF (2000) Yield point spectra for seismic design and rehabilitation. Earthq Spectra 16(2):317–336

ATC (1996) Seismic Evaluation and Retrofit of Concrete Buildings ATC-40. Report No SSC 96-0. Applied technology council/Seismic safety commission, Redwood City, CA

ATC/MCEER (1999) Comprehensive specification for the seismic design of bridges. NCHRP Project 12-49. Applied technology council/multidisciplinary center for earthquake engineering research

Browning JP (2001) Proportioning of earthquake-resistant RC building structures. J Struct Eng 127(2): 145–151

BSSC (1997) NEHRP guidelines for the seismic rehabilitation of buildings, Federal Emergency Management Agency, Washington, D.C., Publication 273

Calvi GM, Kingsley GR (1995) Displacement-based seismic design of multi-degree-of-freedom bridge structures. Earthq Eng Struct Dyn 24:1247–1266

CEN (Comité Europeen de Normalization) (2004) Eurocode 8: design of structures for earthquake resistance—part 1: general rules, seismic actions and rules for buildings. CEN, Brussels

CEN (Comité Europeen de Normalization) (2005) Eurocode 8: design of structures for earthquake resistance—part 2: bridges. CEN, Brussels

Dwairi H, Kowalsky MJ (2006) Implementation of inelastic displacement patterns in direct displacement-based design of continuous bridge structures. Earthq Spectra 22(3):631–662

Freeman SA (1998) The capacity spectrum method as a tool for seismic design. In: 11th European conference on earthquake engineering, Paris, France

Grant DN, Blandon CA, Priestley MJN (2004) Modeling inelastic response in direct displacement-based design. Report No. ROSE 2004/02, IUSS Press, Pavia, Italy

Kowalsky MJ (2002) A displacement-based design approach for the seismic design of continuous concrete bridges. Earthq Eng Struct Dyn 31:719–747

Moehle JP (1992) Displacement-based design of RC structures subjected to earthquakes. Earthq Spectra 8(3):403–428

OpenSees (2006) Open system for earthquake engineering simulation. Available via http://opensees.berkeley.edu. Accessed 30 Oct 2006

Ortiz Restrepo JC (2006) Displacement-based design of continuous concrete bridges under transverse seismic excitation. Masters dissertation, European school for advanced studies in reduction of seismic risk (ROSE School), University of Pavia, Italy

Panagiatakos TB, Fardis MN (1999) Deformation-controlled earthquake-resistant design of RC buildings. J Earthq Eng 3(4):498–518

Priestley MJN (2003) Myths and fallacies in earthquake engineering, Revisited. The Mallet Milne Lecture. IUSS Press, Pavia, Italy

Priestley MJN, Calvi GM (2003) Direct displacement based seismic design of concrete bridges. In: Vth international conference of seismic bridge design and retrofit for earthquake resistance, ACI international conference, La Jolla, California

Priestley MJN, Seible F, Calvi GM (1996) Seismic Design and Retrofit of Bridges. 1. Wiley, New York

Priestley MJN, Calvi GM, Kowalsky MJ (2007) Direct displacement-based design of structures. IUSS Press, Pavia, Italy

Shibata A, Sozen M (1976) Substitute structure method for seismic design in reinforced concrete. J Struct Eng 102(12):3548–3566

Sullivan T (2003) The limitations and performances of different displacement based design methods. J Earthq Eng 7(1):201–241

Uang CM (1991) Establishing R (or R_w) and C_d Factors for Building Seismic Provisions. J Struct Eng 117(1):19–28